



HAL
open science

Cost effective laser structuration of optical waveguides on thin glass interposer

Jean-Marc Boucaud, Folly-Eli Ayi-Yovo, Quentin Hivin, Matthieu Berthomé,
Cédric Durand, Frédéric Giancesello, D. Bucci, Guillaume Ducournau, J.F.
Robillard, Jean-Emmanuel Broquin, et al.

► **To cite this version:**

Jean-Marc Boucaud, Folly-Eli Ayi-Yovo, Quentin Hivin, Matthieu Berthomé, Cédric Durand, et al..
Cost effective laser structuration of optical waveguides on thin glass interposer. *Journal of Lightwave
Technology*, 2017, 35 (20), pp.4445-4450. 10.1109/JLT.2017.2732461 . hal-01961118

HAL Id: hal-01961118

<https://hal.science/hal-01961118>

Submitted on 18 Aug 2022

HAL is a multi-disciplinary open access archive for the deposit and dissemination of scientific research documents, whether they are published or not. The documents may come from teaching and research institutions in France or abroad, or from public or private research centers.

L'archive ouverte pluridisciplinaire **HAL**, est destinée au dépôt et à la diffusion de documents scientifiques de niveau recherche, publiés ou non, émanant des établissements d'enseignement et de recherche français ou étrangers, des laboratoires publics ou privés.

Cost Effective Laser Structuration of Optical Waveguides on Thin Glass Interposer

Jean-Marc Boucaud, Folly-Eli Ayi-Yovo, Quentin Hivin, Matthieu Berthomé, Cédric Durand, Frédéric Giancesello, Davide Bucci, Guillaume Ducournau, Jean-François Robillard, Jean-Emmanuel Broquin, and Emmanuel Dubois

Abstract—In order to enhance electro-optical system-in-package capabilities for silicon photonics, a cost effective fabrication process for optical waveguides integration on thin glass substrate interposer is demonstrated. First, a femtosecond laser ablation coupled with a hydrofluoric acid etching is developed to create microgrooves at the glass surface. Second, a dry film lamination followed by chemical mechanical planarization is achieved to define surface optical waveguides by filling the microchannels. Physical characterizations of the fabricated waveguides are performed using optical and scanning electron microscopy. Finally, optical mode profile and loss characterizations confirm the optical functionality of waveguides which prove to be multimodal at 1550 nm.

Index Terms—Femtosecond laser, polymer optical waveguide, thin glass interposer.

I. INTRODUCTION

FOLLOWING the demand for mobile data, global data center traffic will reach 10 zettabytes (10^{21}) per year in 2019 [1]. Even though optical communication systems in data centers are still widely based on multi-mode VCSEL solutions due to their lower cost for single channel transceivers [2], silicon photonics has emerged as a promising alternative for the industrialisation of high performance and low cost optical transceivers. The interest of silicon photonics is mainly related to mega data centers that need up to 2 kilometer-long connections. Data

This work was supported in part by the STMicroelectronics-IEMN common laboratory, in part by the NANO2017 program, in part by the French government through the National Research Agency (ANR) under program PIA EQUIPEX LEAF ANR-11-EQPX-0025, and in part by the French RENATECH network. (*Corresponding Author: Jean-Marc Boucaud.*)

J.-M. Boucaud, F.-E. Ayi-Yovo, C. Durand, and F. Giancesello are with Technology R&D, STMicroelectronics, 850 rue Jean Monnet, Crolles, 38920, France (e-mail: jean-marc.boucaud@st.com; sfeli.ayiyovo@gmail.com; cedric.durand@st.com; frederic.giancesello@st.com).

Q. Hivin, M. Berthomé, G. Ducournau, J.-F. Robillard, and E. Dubois are with the University of Lille, CNRS, Centrale Lille, ISEN, University of Valenciennes and Hainaut-Cambresis, UMR 8520 IEMN, Lille F-59000, France (e-mail: quentin.hivin@isen.iemn.univ-lille1.fr; matthieu.berthome@isen.iemn.univ-lille1.fr; guillaume.ducournau@iemn.univ-lille1.fr; jean-francois.robillard@isen.iemn.univ-lille1.fr; emmanuel.dubois@isen.iemn.univ-lille1.fr).

D. Bucci and J.-E. Broquin are with IMEP-LaHC, Université de Grenoble Alpes, UMR 5130 CNRS, Minatec-Grenoble-INP, CS 50257, Grenoble 38016, France (e-mail: bucci@minatec.grenoble-inp.fr; broquin@minatec.grenoble-inp.fr).

transfer over extended distances and the increase of aggregated data rate both require single mode fiber connections and opens a market for 4 parallel channels (PSM4) and coarse wavelength division multiplexing (CWDM) applications to achieve 100 and 400 Gb/s optical links. Although considerable achievements have been made in silicon photonics, the coupling scheme between single mode optical fibers and silicon-on-insulator (SOI) waveguides remains a serious challenge. The high index contrast associated to SOI platforms leads to a large mismatch between waveguides and optical fibers, resulting in important coupling losses. Grating Couplers (GCs) [3] are today the most suitable industrial solution, bringing however two majors constraints. Firstly, GCs are very sensitive to fiber misalignment in the micrometer range, thus imposing costly optical active alignment procedures. Secondly, GCs bandwidth is too limited to enable low loss CWDM designs in photonic integrated Circuits (PICs). As a consequence, electro-optical interconnections required to assemble the final module are today far more expensive than the PICs themselves. To cope with the aforementioned problem, several alternative solutions have been proposed in the literature to improve the coupling scheme from the PICs waveguides to fibers in a perspective of cost reduction. For example, optical waveguides forming a multi-rod structure can be made in a spot size converter (SSC) and connected by removing a part of the PIC back-end of line (BEOL) as in [4], or inverted tapers can be structured into the PIC BEOL as in [5]. These solutions properly fix the bandwidth issue by removing the GCs and rely on passive alignment. However, the PIC process has to be modified since no available silicon photonics technology yet supports those proposals while some key challenges are still unaddressed like deep trench in silicon photonics BEOL and organic SSC assembly. In order to keep the currently available silicon photonic technologies, we propose a new approach consisting in the 3D assembly of a PIC on a glass interposer embedding electrical and optical interconnections that is connected to an optical fiber via a passive alignment structure. Optical glass substrates embedding a single mode waveguide technology such as silica-based planar lightwave circuit (PLC) have been demonstrated. In [6], for example, the PLC is used as an interposer for a PIC, which is close to our approach. Another alternative technology is femtosecond laser direct writing of waveguides in glass used in [7]. However electrical interconnections have not been implemented in both technologies. As far as electrical connections are considered, the idea is to leverage current developments performed on thin glass substrates for the high bandwidth memories (HBM) market [8].

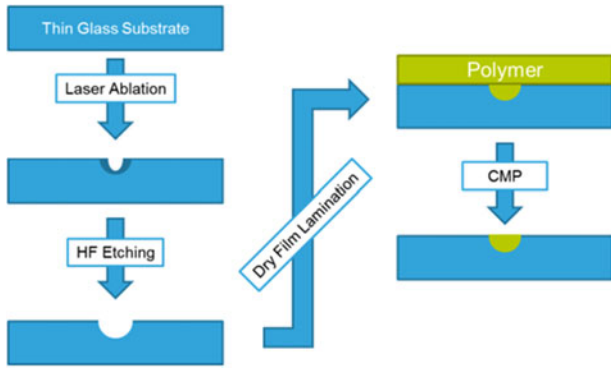


Fig. 1. Fabrication sequence of surface U-shaped optical guide in a thin glass substrate: i) localized laser-induced modification of glass microstructure, ii) U-groove etching based on locally enhanced HF etching rate, iii) dry film polymer lamination to fill the groove and iv) planarization of the core material using CMP.

The pending challenge is therefore to develop cost effective optical interconnections embedded in the glass substrate comprising single mode waveguides and slanted mirrors for the vertical redirection of the beam towards the PIC that is compatible with the fabrication process of electrical redistribution layers on thin glass substrates for HBM. It is worth noting that this strategy enables the reuse of the current PIC design for CWDM based on a wavelength specific GC coupling scheme while athermal multiplexers/demultiplexers are integrated on glass to take advantage of its low thermo-optic coefficients [9]. Moreover, a passive alignment approach could be adopted using a pick-and-place technique with $\sim 1 \mu\text{m}$ alignment accuracy and 3D assembly of fine pitch copper pillars [10]. In that context, the development of optical waveguides using cost effective industrial techniques and tools are of primary relevance. In this paper, we therefore report a new fabrication process of step index polymer optical waveguides using direct laser photo-inscription and etching on thin glass substrates, in order to demonstrate the first building-blocks of a full electro-optical thin glass interposer

II. FABRICATION PROCESS

The complete fabrication sequence involves four elementary steps comprising i) laser modification of glass that locally enhances the etching rate in hydrofluoric (HF) acid, ii) smooth U-shape micro-grooving of glass in HF to delineate the optical guide core, iii) dry film polymer lamination to fill the groove with a high index material and iv) chemical-mechanical polishing to remove the excess of core material. The different steps of the waveguide fabrication process are summarized in Fig. 1. Straight and bent waveguides as well as Y junctions were processed in $500 \mu\text{m}$ thick AF32 Eco Thin Glass 3 inches substrates provided by SCHOTT [16]. To obtain single mode waveguides and a tight coupling with optical fibers at telecom wavelengths, the ideal waveguide core cross-section is targeted to be an $8 \times 8 \mu\text{m}^2$ square with a difference between refractive indexes around 3×10^{-3} .

A. Femtosecond Laser Direct Writing

Over the past decade, femtosecond laser direct writing has emerged as a promising micromachining technique to locally

ablate materials or to structurally change their properties [11]. Furthermore, laser direct writing holds the distinctive advantage of being a maskless technology suitable for fast prototyping loops and does not require operation in clean room conditions, thus reducing complexity and cost. When ultrashort laser pulses propagate in a transparent medium, the extremely high peak power produces spatial self-focusing resulting from the intensity dependence of the refractive index. Above a critical power, a singular wave collapse to a focal point is predicted if self-focusing overcomes diffraction [12] thus leading to the formation of a filament [13], [14]. However, as the pulse grows in intensity, an electron plasma is generated due to non-linear multi-photon and avalanche ionization. This electron gas produces a negative refractive index change that acts as a diverging lens. The laser pulse propagation is therefore governed by a subtle balance between the Kerr focusing, diffraction and defocusing upon coupling with the electron plasma. Depending on the femtosecond laser pulse energy and duration, different types of structural modifications can take place ranging from gentle refractive index variations to material ablation resulting from optical breakdown. Consistently with the above discussion, exposure of glass to a femtosecond laser beam is known to produce a modulation of the refractive index and a dramatic increase of the etching rate in HF acid [15]. In the present work, this last property is used to delineate the U-shaped micro-groove.

The laser setup used to inscribe micro-grooves in glass implements a Tangerine laser source (Amplitude-Systèmes) that provides ~ 350 fs pulses at a wavelength of 343 nm after frequency tripling. The laser beam trajectory is controlled by a galvanometric scanning head equipped with a telecentric lens featuring a focal distance of 100 mm. The focused spot diameter is estimated around $10 \mu\text{m}$ at the considered wavelength. An optical attenuator comprising a half-wave plate and a polarizer allows fine tuning of the beam power independently from the laser source parameters. After running through the entire optical path, the maximum available average power amounts to 2 W at a repetition rate of 200 kHz. Glass inscription was performed under varying operating conditions for the sake of optimization: i) the laser average power was swept from 10 to 100%, ii) the scanning speed was adjusted from 2 to 15 mm/s and iii) the repetition rate was scanned from 10 to 200 kHz.

B. Hydrofluoric Acid Etching

As outlined previously, several types of modifications can occur in glass exposed to femtosecond laser irradiation. The commonly observed structural changes can be classified into three families depending on the pulse energy: i) isotropic increase in refractive index, ii) birefringent modifications and iii) ablation resulting from microexplosions [11]. It is well established that fundamental glass properties like density and refractive index can be associated to the Si-O-Si bond angle [17]. In vitreous silica structures, the short range order is dominated by 6- and 5-membered rings, an n-membered ring being associated to n Si-O segments contained in a closed path. From a minimum-energy standpoint, the formation of 3- and 4-membered rings is not favored because it involves a higher strain energy when compared to their higher order counterparts. A high concentration

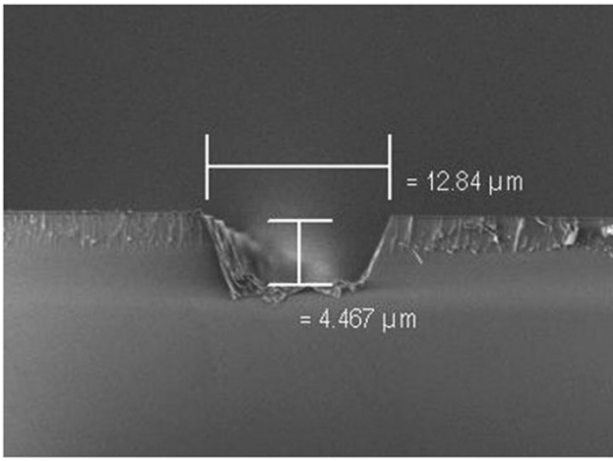


Fig. 2. SEM cross-section of a micro-groove obtained by laser inscription performed with following parameters: repetition rate 30 kHz, average power of 0.12 W, scanning speed of 8 mm/s and HF etching time 2.5 min.

of 3- and 4-membered rings is however possible and is the signature of an out-of-equilibrium state [18] that can typically happen in a quench scenario after laser exposure. This analysis was experimentally consolidated by micro-Raman analysis of glass exposed to femtosecond laser pulses that reveals enhanced Raman peaks at 490 and 605 cm^{-1} that can be assigned to breathing modes of 3- and 4-membered rings [15]. Consistently with the previous analysis, an increased concentration of these rings leads to a global decrease of the average bond angle and, in turn, can be associated to a densified material with higher refractive index. As reported in [12], this structural modification can be accompanied with an accelerated etching rate in HF up to 1:100 with respect to the unexposed material.

In the present study, most laser exposure experiments lead to microexplosions that initiated the formation of narrow channels. At high pulse energy, a channel width around $1\text{ }\mu\text{m}$, much lesser than the spot diameter ($\sim 10\text{ }\mu\text{m}$) suggests that filamentation occurred [19]. Immediately after laser exposure, the depth-elongated form factor resulting from filamentation and remaining glass fragments inside the micro-groove make this structure unsuitable for wave guiding structures. Nevertheless, glass surrounding the micro-grooves in the so-called laser-affected-zone (LAZ) also features an increased refractive index and a marked modifications of its microstructure. To reveal well-formed micro-grooves, the laser-exposed glass samples were dipped in a diluted solution of HF acid (10% HF/H₂O v/v) for relatively short etching times of 2.5 min and 5 min. After rinsing in deionized, samples were cleaned in acetone and isopropanol for 5 min each under ultrasonic agitation. Samples were subsequently diced along a line perpendicular to the laser scan direction to observe the cross-section using scanning electron microscopy (SEM), yielding the typical picture shown in Fig. 2 obtained with the following laser writing conditions: repetition rate of 30 kHz, attenuated average power of 0.12 W, scanning speed of 8 mm/s and HF etching time of 2.5 min.

C. Dry Film Lamination

To fill the micro-groove with a core material, the adopted strategy consists in roll laminating a thin-film polymer available

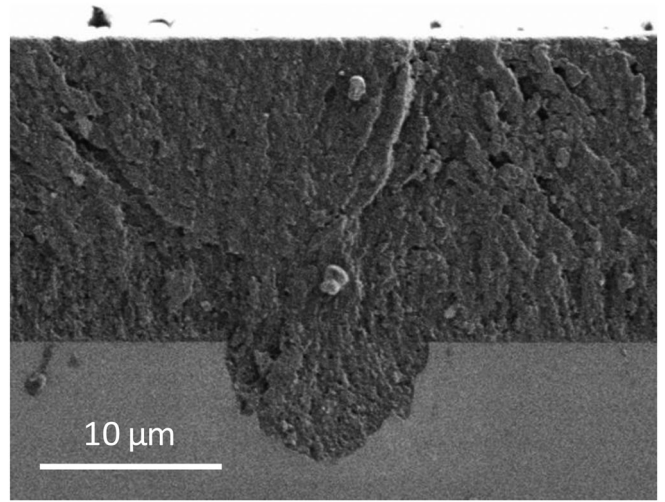


Fig. 3. SEM cross-section of a micro-groove after lamination of an ORDYL SY317 dry film with a roll temperature of $110\text{ }^{\circ}\text{C}$. Five passes of lamination were applied at a pressure corresponding to a static load of 12 kg. A HMDS adhesion promoter was vapor-stream-deposited prior to the dry film application.

under a dry film form. Several constraints apply to the choice of the polymer base material. First, the polymer must exhibit good gap filling properties to conformally shape the geometry of the micro-grooves while remaining stable under varying ambient conditions. Thermosetting resins holds this remarkable property to be initially viscous or soft and to further soften just above its glass transition temperature in such a way that the roll pressure efficiently fills topological inhomogeneities. Providing that the hot lamination temperature reaches glass transition, thermosetting films evolves irreversibly to a cross-linked network characterized by a high level of dimensional stability. The second selection criterion is related to the refractive index of the thermosetting dry film that must be slightly above its AF32 counterpart ($n = 1.4982$ at $\lambda = 1310\text{ nm}$), ideally $\Delta n = 3 \times 10^{-3}$ as stated previously to ensure single mode propagation. Our choice focused on the ORDYL SY317 from ELGA [20] that comes in the form of a $17\text{ }\mu\text{m}$ thick dry film. Although its exact composition is not disclosed by the manufacturer, it is identified as a mix of acrylic polymer and acrylic ester containing the chemically resistant and stable epoxy group [21].

From a practical standpoint, the ORDYL SY317 dry film was laminated with a roll temperature of $110\text{ }^{\circ}\text{C}$. Five passes of lamination were applied at a pressure corresponding to a static load of 12 kg. To improve the bond quality to the glass substrate, an adhesion promoter was applied prior to hot roll lamination. It consists in a very thin layer of hexamethyldisilazane (HMDS) deposited by gaseous streaming on the glass substrate heated to $100\text{ }^{\circ}\text{C}$. The final result is exemplified in Fig. 3 showing the excellent filling of the micro-grooves as well as complete planarization of the dry film top surface.

The refractive index was determined by spectroscopic ellipsometry after lamination onto a non-transparent silicon to facilitate the experimental procedure. Measurements over the $350\text{--}2200\text{ nm}$ wavelength interval were fitted on a simple Lorentz dispersion model [22] with an excellent accuracy. Two application flavors of the dry film were tested covering i) a simple lamination without any post-treatment and ii) a UV

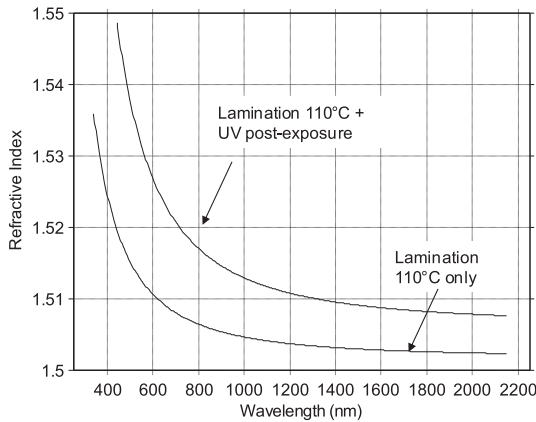


Fig. 4. Refractive index of Ordyl SY317 after 5 passes of hot roll lamination performed at 110 °C. The refractive index can be modulated by post-lamination UV exposure that enhances the cross-linking degree of the polymer typically from 1.503 to 1.510 at a wavelength of 1310 nm.

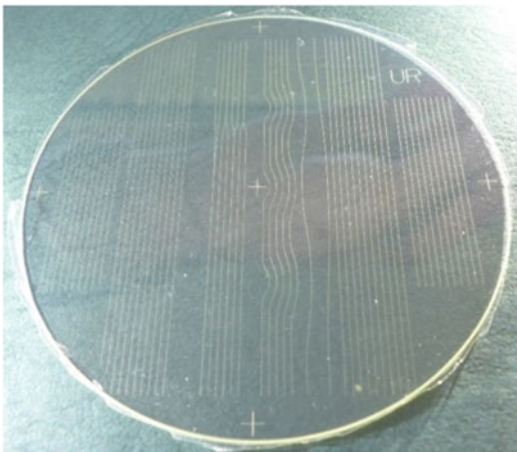


Fig. 5. Picture showing a 3 inches 500 μm thick AF32 Eco glass substrate after laser inscription, HF etching and lamination of a ORDYL SY317 dry film. The layout contains straight and bent waveguides as well as Y junctions.

post-exposure at 365 nm, 10 mW for 60 seconds to evaluate the capability to modulate the refractive index by enhanced cross-linking after hot roll lamination. At a working wavelength of 1310 nm, the dry film core material exhibits a refractive index of 1.503 and 1.510 without and with UV post-exposure, respectively. This results in a core-cladding difference of 0.0048 without UV and 0.0118 with UV cross-linking that does not guarantee the guides to be single mode. However, the immediate availability of the material and its ease of application led us to fabricate the first waveguides. Fig. 5 shows a typical example of AF32 Eco glass substrate after laser inscription, HF etching and ORDYL SY317 lamination. Designed structures comprising straight, bent and Y junction waveguides can be clearly identified.

D. Chemical Mechanical Polishing

As exemplified in Fig. 3, the dry film thickness largely exceeds the depth of the processed micro-grooves which prevents proper confinement for light guiding. In order to remove the

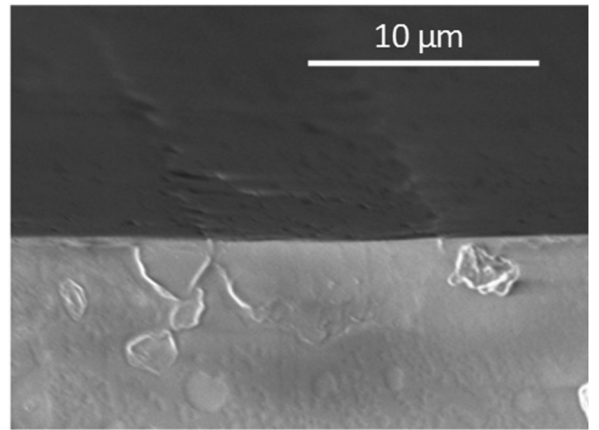


Fig. 6. SEM picture showing a cross-section of a surface waveguide after the CMP step. The core hemicylinder is composed of ORDYL SY317, the bottom cladding is a glass substrate AF32 Eco.

excess of polymer to delineate a surface waveguide, chemical mechanical polishing (CMP) has been used. CMP is well established in the semiconductor industry to achieve global surface planarization in complex stack of interconnection layers [23]. One major challenge of this technique is to avoid layer delamination due to the high-torque nature of the polishing mechanism [24]. This remark is all the more true that polymers have typically a lower elastic modulus and hardness when compared to metals and other inorganic dielectrics like silicon oxide or nitride. As a result, polymers are more prone to delamination, tearing and a source of scrap residues. To circumvent this difficulty, ORDYL SY317 was systematically exposed to UV to produce a highly cross-linked layer that is more robust to withstand high pressures and frictions during the CMP process.

As most polymers are generally resistant to acidic and basic solutions, it can be expected that the removal rate of polymer is dominated by the mechanical action rather than the chemical one. Our choice of polishing slurry and pad was therefore guided to keep a high degree of compatibility with glass to guarantee a high removal rate contrast between the polymer and the supporting glass substrate. For that sake, a colloidal silica based slurry with basic pH and particle size of 70 nm was used for its proven affinity with silicon dioxide that we assume to be the same with glass. A soft polyurethane impregnated polyester felt was used as polishing pad to ensure a high precision surface finish. Among other parameters, the pressure and rotation speed of the polishing head as well as the spinning speed of the pad plate are critical parameters that strongly condition the quality of planarization. Fig. 6 shows a typical result obtained with a carrier pressure of 1200 mda N/cm², a substrate blowing back pressure of 600 mda N/cm² and the same rotation speed of 60 rpm for the carrier and the pad plate. Based on this approach, we successfully managed to planarize the polymer overlayer without noticeable dishing, hence creating surface waveguides.

III. OPTICAL CHARACTERIZATION

Several samples were fabricated following the previously described process, then cleaved and characterized by three

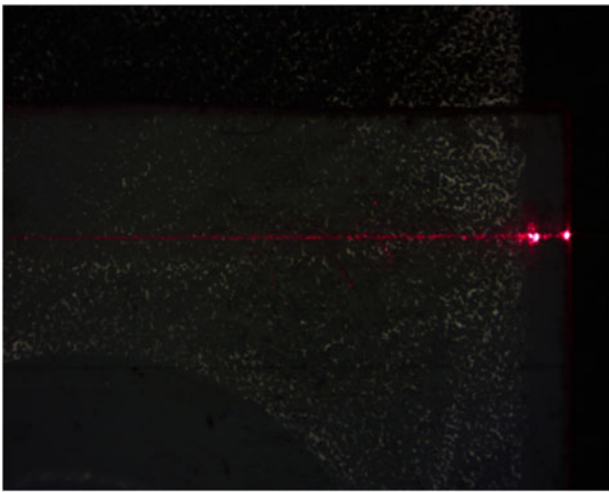


Fig. 7. Top view of the waveguide during characterization in the visible spectrum.

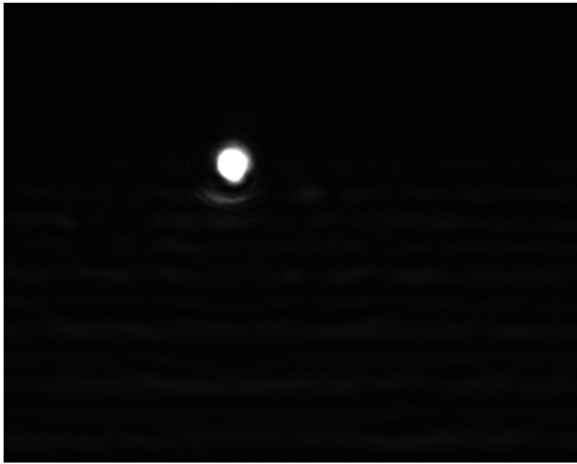


Fig. 8. Mode profile of a waveguide at 1550 nm.

different methods. The first characterization was made in the visible spectrum, near 650 nm, and an optical fiber on a XYZ positioning stage is carefully aligned in front of the optical waveguide. If the waveguide contains discontinuities, they will appear in the light scattered and will become visible by observing the waveguide from above. As shown in Fig. 7, the light is propagating through the waveguides despite reflection at the facet where light was injected and regular discontinuities, probably due to some material degradation attributed to the cleaving process.

The second type of characterization was carried out to determine the mode profile. We used a light source at a wavelength of 1550 nm and a fiber optic for light injection. The light at the output of the waveguides is focused on an infrared camera by means of a microscope objective. By properly aligning the injection fiber, mode profiles were observable as shown in Fig. 8. The waveguide is considered to be multimode since modal interferences are visible by moving the injection fiber. Finally, the microscope objective and the infrared camera were removed and replaced by an output fiber to evaluate the optical losses of

a 2 cm long waveguide at 1550 nm. We measured 26 dB of total insertion losses, which include reflections at the input and the output of the waveguide, coupling between the optical fiber and the waveguide modes propagation losses.

IV. CONCLUSION AND PERSPECTIVES

We developed an innovative fabrication process of polymer waveguides that could be integrated on thin glass interposer using femtosecond laser inscription, HF acid etching, dry film lamination and CMP. Waveguides manufactured following this process have demonstrated guiding properties despite being multimode and having high losses. However, this fabrication process has many advantages over mainstream technologies: i) it does not involve masking steps, nor require clean room environment, ii) it gives the possibility of tuning the refractive index to select the propagation mode size and is compatible with the recent developments of electrical glass interposers. It also appears as simpler from the process complexity standpoint when compared with silica-based PLCs that relies on flame hydrolysis deposition and reactive ion etching [25]. Another distinctive advantage is that the present approach does not depend on the optical properties of a single material as it is the case in direct writing of waveguides using femtosecond inscription [26]. Future works will further develop the process to obtain single mode propagation conditions and reduce losses in order to become competitive with existing optical waveguide technologies.

REFERENCES

- [1] Cisco, "Cisco global cloud index: Forecast and methodology, 2014–2019," Cisco, San Jose, CA, USA, White Paper, Apr. 2016.
- [2] D. Mahgerefteh *et al.*, "Techno-economic comparison of silicon photonics and multimode VCSELs," *J. Lightw. Technol.*, vol. 34, no. 2, pp. 233–242, Jan. 2016.
- [3] F. E. Ayi-Yovo *et al.*, "Enablement of advanced silicon photonics optical passive library design leveraging silicon based RF passive development methodology," in *Proc. 16th Topical Meet. IEEE Silicon Monolithic Integr. Circuits RF Syst.*, Austin, TX, USA, 2016.
- [4] M.-J. Picard, Y. Painchaud, C. Latrasse, C. Larouche, F. Pelletier, and M. Poulin, "Novel spot-size converter for optical fiber to sub- μm silicon waveguide coupling with low loss, low wavelength dependence and high tolerance to alignment" in *Proc. Eur. Conf. Opt. Commun.*, Valencia, Spain, 2015.
- [5] N. Hatori *et al.*, "A novel spot size converter for hybrid integrated light sources on photonics-electronics convergence system," in *Proc. 9th Int. Conf. Group IV Photon.*, San Diego, CA, USA, 2012.
- [6] K. Watanabe, A. Leinse, D. Van Thourhout, R. Heideman, and R. Baets, "Silica-based optical interposer for Si photonics" in *Proc. Eur. Conf. Lasers Electro-Opt. Quantum Electron.*, Munich, Germany, 2009.
- [7] M. Mirshafiei, J.-P. Berub, S. Lessard, R. Vall, and D. V. Plant, "Glass interposer for short reach connectivity," *Opt. Express*, vol. 24, no. 11, pp. 12375–12384, 2016.
- [8] T. Sakai *et al.*, "Design and demonstration of large 2.5D glass interposer for high bandwidth applications," in *Proc. Int. Symp. IEEE CPMT Jpn.*, Kyoto, Japan, 2014.
- [9] C. R. Doerr, M. Cappuzzo, L. Gomez, E. Chen, A. Wong-Foy, and E. Laskowski, "Planar lightwave circuit eight-channel CWDM multiplexer," in *Proc. Int. Conf. Opt. Fiber Commun.*, Los Angeles, CA, USA, 2004.
- [10] V. Smet *et al.*, "Interconnection materials, processes and tools for fine-pitch panel assembly of ultra-thin glass substrates," in *Proc. Int. Conf. Electron. Compon. Technol.*, San Diego, CA, USA, 2015.
- [11] R. Osellame, G. Cerullo, and R. Ramponi eds., *Femtosecond Laser Micro-machining: Photonic and Microfluidic Devices in Transparent Materials*. New York, NY, USA: Springer, 2012.

- [12] C. B. Schaffer, A. Brodeur, and E. Mazur, "Laser-induced breakdown and damage in bulk transparent materials induced by tightly focused femtosecond laser pulses," *Meas. Sci. Technol.*, vol. 12, pp. 1784–1794, 2001.
- [13] K. D. Moll and A. L. Gaeta, "Self-similar wave collapse: Observation of the townes profile," *Phys. Rev. Lett.*, vol. 90, no. 20, 2003, Art. no. 203902.
- [14] Y. Bellouard, A. Said, M. Dugan, and P. Bado, "Fabrication of high-aspect ratio, micro-fluidic channels and tunnels using femtosecond laser pulses and chemical etching," *Opt. Express*, vol. 12, no. 10, pp. 2120–2129, 2004.
- [15] J. W. Chan, T. Huser, S. Risbud, and D. M. Krol, "Structural changes in fused silica after exposure to focused femtosecond laser pulses," *Opt. Lett.*, vol. 26, pp. 1726–1728, 2001.
- [16] AF32 Eco Thin Glass datasheet. [Online]. Available: http://www.schott.com/advanced_optics/english/download/schott-af-32-eco-thin-glass-may-2013-eng.pdf
- [17] A. Masuno, N. Nishiyama, F. Sato, N. Kitamura, T. Taniguchi, and H. Inouea, "Higher refractive index and lower wavelength dispersion of SiO₂ glass by structural ordering evolution via densification at a higher temperature," *RSC Adv.*, vol. 6, pp. 19144–19149, 2016.
- [18] A. Pasquarello and R. Car, "Identification of Raman defect lines as signatures of ring structures in vitreous silica," *Phys. Rev. Lett.*, vol. 80, no. 23, pp. 5145–5147, 1998.
- [19] L. Bergé, S. Skupin, R. Nuter, J. Kasparian, and J. P. Wolf, "Ultrashort filaments of light in weakly ionized, optically transparent media," *Rep. Progress Phys.*, vol. 70, pp. 1633–1713, 2007.
- [20] ORDYL SY300 dry films. [Online]. Available: <http://www.elgaeurope.it/en>
- [21] P. Vulto *et al.*, "Microfluidic channel fabrication in dry film resist for production and prototyping of hybrid chips," *Lab Chip*, vol. 5, pp. 158–162, 2005.
- [22] M. Born and E. Wolf, *Principles of Optics*. 7th ed. Cambridge, U. K.: Cambridge Univ. Press, 1999, Ch.2.
- [23] P. B. Zantyea, A. Kumara, and A. K. Sikderb, "Chemical mechanical planarization for microelectronics applications," *Mater. Sci. Eng. R*, vol. 45, pp. 89–220, 2004.
- [24] S. Balakumar *et al.*, "Peeling and delamination in Cu/SiLK process during Cu-CMP," *Thin Solid Films*, vol. 462–463, pp. 161–167, 2004.
- [25] A. Himeno, K. Kato, and T. Miya, "Silica-based planar lightwave circuits," *IEEE J. Sel. Topics Quantum Electron.*, vol. 4, no. 6, pp. 913–924, Nov./Dec. 1998.
- [26] K. Miura, J. Qiu, H. Inouye, T. Mitsuyu, and K. Hirao, "Photowritten optical waveguides in various glasses with ultrashort pulse laser," *Appl. Phys. Lett.*, vol. 71, 1997, Art. no. 3329.